



Cite this: *Phys. Chem. Chem. Phys.*,  
2017, **19**, 19640

## Energy flow in peptides after UV photoexcitation of backbone linkages†

Klavs Hansen,<sup>\*abc</sup> Camilla Skinnerup Byskov<sup>b</sup> and Steen Brøndsted Nielsen<sup>id</sup> <sup>\*bd</sup>

We report on the dissociation channels after UV photoexcitation of peptide cations tagged with 18-crown-6 ether (CE). The model peptides chosen for study were singly protonated (Ala)<sub>n</sub>-Pro (*n* = 1, 2, 3) and Pro-Pro (Ala = alanine, Pro = proline) that all contain at least one tertiary amide group with high absorption cross section at 210 nm (5.90 eV). Statistical dissociation was identified from the loss of CE, a process occurring remotely from the initial site of excitation, and therefore requiring flow of energy to the ammonium group where the CE is bound. However, homolytic breakage of the peptide backbone at the site of excitation is competitive, resulting in so-called *a* radical cations. Density functional theory calculations of dissociation energies were done on the simplest system [Ala-Pro + H<sup>+</sup>](CE) and found to be 1.87 eV for CE loss and 3.29 eV for the formation of *a*<sup>+</sup>(CE) and *x*. These numbers were used to calculate statistical branching ratios for the dissociation processes based on detailed balance. After the absorption of two 210 nm photons (according to power-dependence measurements), the branching ratio between the two channels is calculated to be less than 10<sup>-4</sup>, far below the observed ratio of 0.65. Hence both statistical and non-statistical dissociation contribute to dissociation of these photoexcited peptides.

Received 20th March 2017,  
Accepted 28th April 2017

DOI: 10.1039/c7cp01768e

rsc.li/pccp

## Introduction

Photo-induced dissociation (PID) of peptides and proteins in combination with mass spectrometry has in recent years become an important supplement to other techniques (*e.g.*, collision-induced dissociation (CID) and electron-transfer dissociation (ETD)) for peptide sequencing.<sup>1–3</sup> In most experiments, either 157 nm (7.9 eV) photons from an F<sub>2</sub> excimer laser or 193 nm (6.4 eV) photons from an ArF laser were used to excite amide chromophores. The energy absorbed is far more than typical peptide bond strengths (3–4 eV). It should also be mentioned that significant work has been done on protonated aromatic amino acids and peptides containing such UV chromophores.<sup>4–8</sup> PID has also been used in combination with ETD to provide more detailed information on the structure of the fragment ions and isomerization processes.<sup>9</sup> PID benefits in comparison to CID by not changing the pressure in the mass spectrometer and provides a well-defined amount of excitation energy. However, the actual mechanism for dissociation is still not well understood and

has been up for much debate since the very first PID experiments on peptides by McIver and co-workers<sup>10</sup> in the 1980s.

Information on the energy flow processes within the peptide after photoexcitation is necessary to properly understand the dissociation mechanism, and whether it is statistical or not. Statistical implies here that the excitation energy is randomized over all degrees of freedom prior to dissociation so all memory of the initial excited state is lost, except for the conserved quantities: energy, momentum and angular momentum. Of particular importance for the use of PID to pinpoint posttranslational modifications<sup>3</sup> is the information whether or not cleavage occurs at the initial site of excitation as rearrangements could occur if the dissociation is slow and statistically.

It can, however, be difficult, if not impossible, from the dissociation channels themselves to distinguish between statistical and prompt dissociation. This is certainly the case if the channels are the same for direct and delayed dissociation. In the case of a vibrationally hot peptide cation, the ionizing proton becomes mobile and moves to an amide group where it lowers the C(O)–N dissociation energy.<sup>11</sup> This same bond could be broken in a prompt dissociation process. In a previous publication, we suggested a method to disentangle the two channels based on photodissociation of peptide cations tagged with 18-crown-6 ether (CE).<sup>12</sup> The CE is bound to an ammonium group that is remotely located with regard to the site of photoexcitation. We chose peptides containing one or more proline residues to have high oscillator strengths in the ultraviolet region. A tertiary amide (*i.e.*, involving a proline linkage) has

<sup>a</sup> Tianjin International Center of Nanoparticles and Nanosystems, Tianjin University, 92 Weijin Road, Nankai District, Tianjin 300072, P. R. China. E-mail: klavshansen@tju.edu.cn

<sup>b</sup> Department of Physics and Astronomy Aarhus University, DK-8000 Aarhus C, Denmark. E-mail: sbn@phys.au.dk

<sup>c</sup> Department of Physics, University of Gothenburg, 41296 Gothenburg, Sweden

† Electronic supplementary information (ESI) available: Calculated structures, vibrational frequencies, zero-point energies, single-point energies, and more details on the calculations of rate constants. See DOI: 10.1039/c7cp01768e

an absorption cross section that is three times larger than that of a secondary amide (at 214 nm),<sup>13</sup> and we therefore have some control over where we initially deposit the photon energy. We found that the dominant channel after photoexcitation of CE-tagged peptides was loss of CE (*i.e.*, statistical dissociation) but also that some rupture of the peptide backbone occurred (scission of C<sub>α</sub>-C(O) or C(O)-N bonds) to give a series of *a*, *x* and *b*, *y* fragments and ascribed this to prompt breakage of the backbone. Also side-chain cleavages were seen.

The CE is not only important for the question of statistical dissociation, it also immobilizes the ammonium protons thereby preventing a proton to move to an amide group and lower the dissociation energy for backbone cleavage (*cf.*, the mobile proton model mentioned above).

To investigate further the reality of non-statistical breakage of the peptide backbone, we have in this work studied simpler peptides that in addition to proline contain alanine. In the case of the smallest one, [Ala-Pro + H<sup>+</sup>](CE), we did density functional theory calculations of dissociation energies and used these to calculate approximate rate constants for the dissociation channels, enabling us to quantify the expected branching ratio in a statistical decay.

## Experimental

The setup used for the PID experiments has been described in detail elsewhere,<sup>14,15</sup> and only a brief description will be given here. 18-Crown-6 ether was purchased from Sigma-Aldrich and synthetic peptides from LifeTein LLC (Hillsborough, NJ, USA). Both peptide and CE were added to a water/methanol (1:1) solution with 10% acetic acid in volume and electrosprayed to produce complexes between protonated peptides and CE. All ions were accumulated in an octopole trap that was emptied at a frequency of 40 Hz. After acceleration to 50 keV kinetic energies of the singly charged ions, they were mass selected by an electromagnet, followed by laser irradiation. Only every second ion bunch was irradiated to correct for dissociation not due to photoexcitation. The laser system is a 20 Hz Nd:YAG where the third harmonic is pumping an optical parametric oscillator to produce 420 nm blue light (and 2300 nm infrared light). The blue light was then frequency doubled in a barium borate (BBO) crystal to produce the 210 nm UV light. Finally, a hemispherical electrostatic analyzer was used to mass-separate the fragment ions that were counted with a channeltron detector. To obtain the PID spectrum, the difference between the laser-on and laser-off signals was taken. Synchronization and timing of each step in the experiment were done with a Labview program.

## Calculations

### Dissociation energies

All structure calculations were done with the Gaussian-03W program.<sup>16</sup> Geometries were optimized at the B3LYP/6-31G(d) level of theory, and frequencies were calculated to verify that the structures are not saddle points. Single point calculations

were done at a higher level, B3LYP/6-311++G(2d,p). All energies were corrected for zero-point kinetic energies (harmonic oscillator approximation). Dissociation energies were obtained from the energy difference between products and the reactant (*i.e.*, [Ala-Pro + H<sup>+</sup>](CE)).

### Rate constants

The calculation of rate constants was done with the detailed balance formalism.<sup>17</sup> As in the more familiar RRKM formalism,<sup>18</sup> it involves the ratio of level densities of reactant and products. Relative to the simplest version, describing evaporation of a single atom, it requires modification for an evaporated fragment with internal degrees of freedom, primarily vibrations and the rotations. To the extent that the excitation energy of the dissociated system can be separated into the vibrational and rotational components, we have (the relative translational kinetic energy of the two fragments can be ignored in this connection),

$$E_{\text{exct}} = E - \Delta E = E_{\text{rot}} + E_{\text{vib}},$$

$E$  is the excitation energy of the parent ion (initial energy plus photon energy), and  $\Delta E$  is the dissociation energy. It is possible to incorporate the vibrational and rotational degrees of freedom into the rate constant. This is accomplished by integrating over the partitioning of the energy over the two fragments. For the vibrations the procedure is simple, because it gives the vibrational level density of the whole fragment system after dissociation.<sup>19</sup> The Beyer-Swinehart algorithm was used for these calculations.<sup>20</sup> The rotational degrees of freedom carry only a minor amount of excitation energy. This simplifies the calculation of the product level density, which is also a convolution:<sup>19</sup>

$$\rho(E - \Delta E) = \int_0^{E - \Delta E} \rho_{\text{vib}}(E - \Delta E - E_{\text{rot}}) \rho_{\text{rot}}(E_{\text{rot}}) dE_{\text{rot}},$$

The simplification consists in expanding the logarithm of the vibrational degrees' of freedom level density

$$\rho_{\text{vib}}(E - \Delta E - E_{\text{rot}}) = \rho_{\text{vib}}(E - \Delta E) \exp\left(-\frac{E_{\text{rot}}}{k_{\text{B}} T}\right),$$

where  $k_{\text{B}} T$  is defined as the reciprocal of the first order derivative of the logarithm of the level density (see ref. 19 for more details). The integral then yields the canonical partition function for the rotational degrees of freedom, and the inclusion of rotations is then simply achieved by multiplication with the canonical rotational partition function,  $Z_{\text{rot}}$ , evaluated at the product microcanonical temperature:

$$\rho(E - \Delta E) = Z_{\text{rot}}(T) \rho_{\text{vib}}(E - \Delta E)$$

The rotational partition function involves the rotation of both fragment species. Due to conservation of angular momentum, these cannot be integrated over separately, and the partition function is therefore not the product of the two partition functions, but rather reduces to a single partition function. The issue is complicated by the fact that the capture cross section for the inverse process, needed to calculate the rate constants, also involves integration over angular momenta, defined by

the impact parameter and the momentum in that channel. The resulting final theory is not yet available. As a physically motivated solution we will (1) take the inverse process capture cross section to be geometric for both observed processes and identical in magnitude, and (2) use the sum of the reciprocal geometric averages of the moments of inertia of the two fragments  $I_1$ ,  $I_2$  as the effective moment of inertia  $I_{\text{eff}}$ ,

$$\frac{1}{I_{\text{eff}}} = \frac{1}{I_1} + \frac{1}{I_2}$$

The rotational partition function is then calculated with this moment of inertia in the semiclassical approximation. The moments of inertia along the principal axes (for the common isotopes) are equal to (all in units of  $u \text{ \AA}^2$ ) 247.27, 441.89, 561.51, and 813.80, 928.06, 1624.2 for the crown ether loss, and 148.30, 236.49, 310.11 and 947.06, 1077.3, 1646.2 for the peptide bond break. This gives the two effective rotational temperatures of 0.298 K for the crown ether loss and 0.460 K for the peptide bond breaking. The microcanonical temperatures of the products are 982 K and 876 K. This gives the semiclassical rotational partition functions  $Z_{\text{rot}}$  of 335 000 and 147 000 for the two fragment systems, *i.e.*, a significant enhancement relative to a simple transition state theory calculation.

The assumption of a geometric attachment cross section seems to ignore important steric factors. We believe these factors are absent and the geometric cross section expected to be a good approximation because a complex formed by soft collisions will likely have a sufficiently long lifetime to reach the ground-state geometry before re-evaporation, as illustrated schematically in Fig. 1 (no bond-breaking is required for the rearrangement). It is very possible and probably unavoidable that the complex will experience metastable configurations when diffusing around on the phase space surface. These states are not expected to be long-lived because the total excitation energy is 12.5 eV and the fragments are attracted by relatively weak van der Waals forces, rendering minima relatively shallow compared to the effective temperature and the barrier hopping attempt on the order of the vibrational frequency. In summary, when one forms the ratio of two different rate constants that involve fragments of similar size, mass, and disintegration energy, the factors involving angular momentum, fragment masses *etc.* tend to cancel. We can therefore calculate the

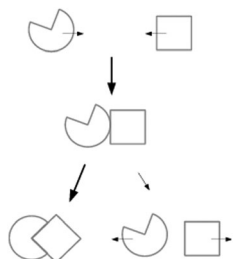


**Fig. 1** An illustration of the inverse, two-step attachment process, with the competing re-evaporation process indicated for the second step. The barriers for rearrangements are expected to be lower than for re-evaporation, making the minimum energy configuration search efficient.

branching ratio BR, which is the ratio of rate constants, as the ratio of product vibrational level densities, *i.e.*,

$$\text{BR} = \frac{\rho_1(E - \Delta E_1)}{\rho_2(E - \Delta E_2)}$$

where the subscripts refer to the channel considered ((1) homolytic bond breakage and (2) CE loss).

Keeping the systematic uncertainty concerning the rotational motion in mind, we can calculate the rate constant for crown ether loss, assuming that the rotational degrees of freedom are taken into account by multiplication of the rate constants by the classical rotational partition functions at the relevant temperature, which is the product temperature given above. This factor is set to the calculated value of  $10^6$ .

## Results and discussion

### PID mass spectra

Photoexcitation of the bare, singly protonated Ala-Pro peptide leads to several different fragment ions (Fig. 2a) and is in accordance with previously published PID spectra.<sup>1–3,10,12</sup> Dominant fragment ions are  $a^+$  and  $y^+$ , loss of COOH or  $\text{H}_2\text{O}$  from  $y^+$ , as well as loss of COOH/HCOOH from the parent peptide followed by loss of  $\text{NH}_3$  (see nomenclature in Fig. 2). In contrast, the PID spectrum of  $[\text{Ala-Pro} + \text{H}^+](\text{CE})$  is much simpler with two dominant channels corresponding to the formation of the bare peptide ( $[\text{Ala-Pro} + \text{H}^+]$ ) and CE and the formation of  $a^+(\text{CE}) + x$ , the latter with an intensity of 0.65 relative to the former. A minor peak is ascribed to loss of COOH/HCOOH from the parent complex; it amounts to 0.12 relative to the CE loss channel. This channel may arise from

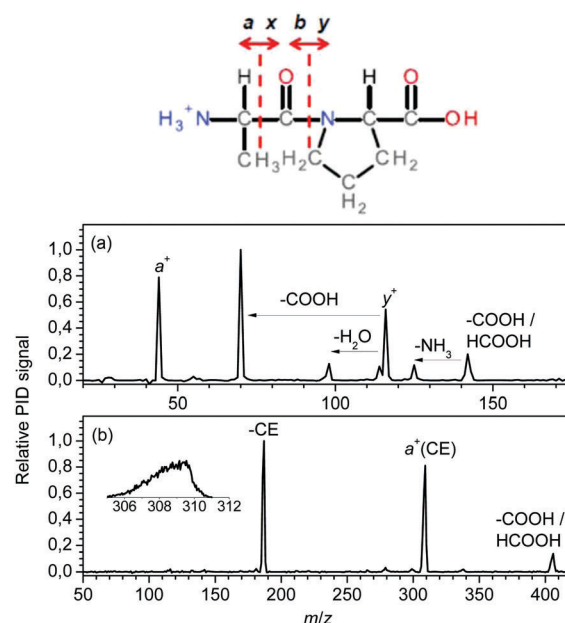


**Fig. 2** PID mass spectra of (a)  $[\text{Ala-Pro} + \text{H}^+]$  and (b)  $[\text{Ala-Pro} + \text{H}^+](\text{CE})$ . The inset shows a zoom-in on the  $a^+(\text{CE})$  peak. The structure of the peptide is shown at the top including the nomenclature for the backbone fragment ions.

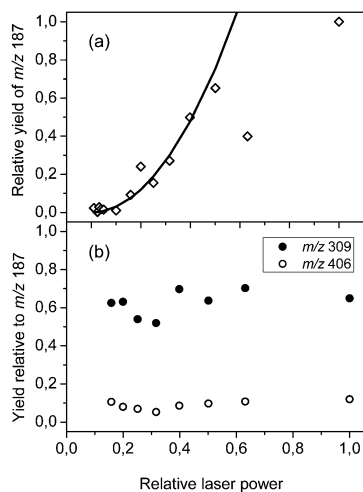


**Fig. 3** (a) Yield of  $[\text{Ala-Pro} + \text{H}^+]$  ( $m/z$  187) after photoexcitation of  $[\text{Ala-Pro} + \text{H}^+](\text{CE})$  versus relative laser power (1 is maximum power). A  $x^2$  function was fit to the data points at low laser power. (b) Yields of  $a^+(\text{CE})$  ( $m/z$  309) and  $[\text{Ala-Pro} + \text{H}^+](\text{CE}) - \text{COOH}$  ( $m/z$  406) relative to  $[\text{Ala-Pro} + \text{H}^+]$  versus relative laser power.

direct excitation of the carboxylic acid group which occurs with a lower cross section than the excitation of the amide group.<sup>12</sup> The  $a^+(\text{CE})$  peak is broadened towards lower masses which implies that in addition to homolytic bond dissociation some H-transfer also takes place between the two fragments to give  $[a^+ - \text{H}](\text{CE})$  together with the neutral fragment  $[x + \text{H}]$ . According to power-dependence measurements, more than one photon is required for the loss of CE (Fig. 3a). At low laser powers, dissociation is in accordance with the absorption of two photons. At higher laser powers, saturation occurs as all the ions in the interaction region have absorbed two photons, and yields no longer follow single power laws. The two photon threshold is consistent with the expectation from the calculations of the rate constants (*vide infra*), even if reservations concerning the accuracy of the absolute values remain. The yield of the other two fragment ions ( $a^+(\text{CE})$  and  $[\text{Ala-Pro-H}^+](\text{CE}) - \text{COOH}$ ) relative to  $[\text{Ala-Pro-H}^+]$  is independent of laser power (Fig. 3b), which implies that the same number of photons account for each of the three dissociation channels (two photons).

The experiment was repeated for other peptides,  $[\text{Pro-Pro} + \text{H}^+](\text{CE})$  (Fig. 4) and  $[\text{Ala-Ala-Pro} + \text{H}^+](\text{CE})$  and  $[\text{Ala-Ala-Ala-Pro} + \text{H}^+](\text{CE})$  (Fig. 5). In the former case, the PID spectrum of the bare peptide,  $[\text{Pro-Pro} + \text{H}^+]$  is simple, giving one dominant fragment ion,  $a^+$ , and minor intensities assigned to  $y^+$  and ions that have lost either COOH or HCOOH. In the case of the complex with CE, loss of CE is dominant but the formation of  $a^+(\text{CE})$  is again significant.

For the two larger peptides, loss of CE is dominant but now there are more backbone cleavages as the peptide contains two and three amide linkages, respectively. Interestingly, in the case of  $[\text{Ala-Ala-Pro} + \text{H}^+](\text{CE})$ , the relative ratio between the  $a_2^+(\text{CE})$  and  $a_1^+(\text{CE})$  (subscripts refer to the number of residues in the fragment) peaks is about 3 : 1, similar to the difference in absorption cross section between the two amide linkages (the amide linkage

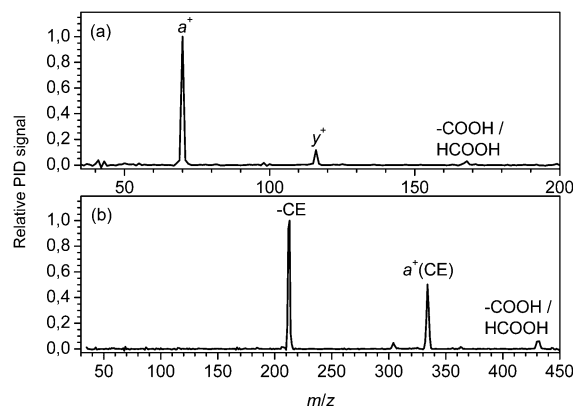


**Fig. 4** PID mass spectra of (a)  $[\text{Pro-Pro} + \text{H}^+]$  and (b)  $[\text{Pro-Pro} + \text{H}^+](\text{CE})$ .

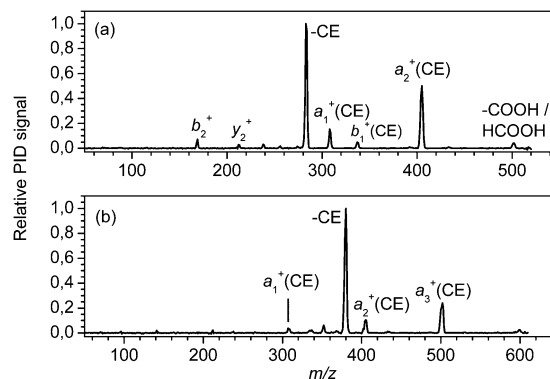


**Fig. 5** PID mass spectra of (a)  $[\text{Ala-Ala-Pro} + \text{H}^+](\text{CE})$  and (b)  $[\text{Ala-Ala-Ala-Pro} + \text{H}^+](\text{CE})$ .

between Ala and Ala is secondary while the one between Ala and Pro is tertiary). Likewise, the peak due to the  $a_3^+(\text{CE})$  ion formed from  $[\text{Ala-Ala-Ala-Pro} + \text{H}^+](\text{CE})$  is larger than those corresponding to  $a_2^+(\text{CE})$  and  $a_1^+(\text{CE})$ . These observations are consistent with prompt dissociation though not directly a proof of it.

The branching ratio between peptide backbone cleavage and loss of CE is different for the different peptides under study as was also seen previously.<sup>12</sup> Including the previous work, we have studied a total of nine peptides where the branching ratio varies between 0.2 and 0.8. The excitation energy per degree of freedom would vary significantly between the peptides as they are composed of different amino acids and the number of residues was 2, 3 or 4. Furthermore, there would be small variations in the energy needed for the homolytic bond breakages as well as for CE loss. It is therefore remarkable that the variation in branching ratio is not larger than it is; this fact is difficult to reconcile with pure statistical dissociation, again pointing to a significant contribution from direct light-induced bond-breaking.

In other experiments, the excitation energy was initially deposited in the indole group of tryptophan and not in the amide group, which reduced the branching ratio to 0.04.<sup>12</sup> In low-energy CID experiments there was no sign of backbone cleavage as long as the protons were sequestered at the ammonium group by the CE.<sup>12</sup> Taken together, all our experimental

data indicate that the breakage of the peptide backbone is prompt after UV excitation of an amide group, and that statistical dissociation favors CE loss by far over backbone cleavage. Basically, it matters how the energy is supplied. In the following, we provide the quantum chemical background for the miscellaneous energies and vibrational frequencies used to reach this conclusion.

### Calculational results

Electronic structure calculations were done for  $[\text{Ala-Pro} + \text{H}^+](\text{CE})$  and the dominant fragment ions according to the PID mass spectrum. We find that loss of CE requires 1.87 eV at the B3LYP/6-311++G(2d,p)//B3LYP/6-31G(d) level of theory, which is in good agreement with previous calculations (1.80 eV and 1.96 eV for the loss of CE from singly protonated diaminoheptane at the B3LYP/6-31+G(d,p) and B3-PMP2/6-311++G(2d,p) levels of theory, respectively).<sup>21</sup> Homolytic breakage of the peptide backbone to give  $a^+(\text{CE})$  and  $x$  fragments is associated with an energy cost of 3.29 eV, nearly 1.5 eV more than that of CE loss. The formation of  $[a - \text{H}]^+$  and  $[x + \text{H}]$  costs only 1.03 eV, and H-transfer between  $a^+$  and  $x$  fragments is therefore favorable, accounting for the large  $[a - \text{H}]^+$  peak in the PID mass spectrum (shoulder to lower masses). The calculated structures are shown in Fig. 6. It should be mentioned that there are likely many different initial structures of the  $[\text{Ala-Pro} + \text{H}^+](\text{CE})$  parent ion, which would give some variations in the reaction energies. However, the presence of such structures will not significantly change the dissociation rate constants in the statistical regime. They will mainly have consequences for a hypothetical chemical equilibrium situation (for a detailed discussion of this question, see ref. 22).

The rate constant for CE loss as a function of excitation energy is shown in Fig. 7; for the calculation the activation energy was assumed identical to the dissociation energy (1.87 eV). The experimental time window for dissociation is up to about 10  $\mu\text{s}$  after photoexcitation, which implies limited dissociation after the absorption of one 210 nm (5.90 eV) photon according to the calculated rate constants. To reach a rate constant of  $10^5 \text{ s}^{-1}$  requires excitation energies of about 6.9 eV. On the other hand, the absorption of two 210 nm photons would basically give complete dissociation on the experimental time scale, in agreement with the power dependence measurement. We used a similar approach to calculate the rate constant for the formation of  $a^+(\text{CE})$  and  $x$ , again equating the activation

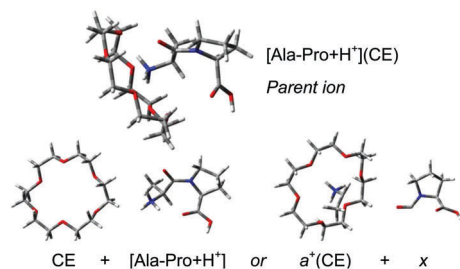


Fig. 6 Calculated structures relevant for the two dissociation processes that we compare in this work.

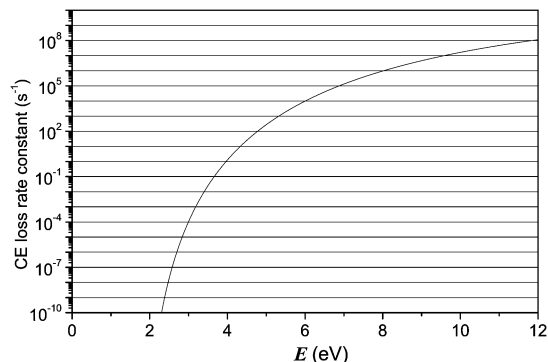


Fig. 7 Calculated rate constant for CE loss from  $[\text{Ala-Pro} + \text{H}^+](\text{CE})$  versus excitation energy. A rotational enhancement factor of  $10^6$  was used. The experimental time window for dissociation is up to about 10  $\mu\text{s}$ , which implies limited dissociation after the absorption of one 210 nm (5.90 eV) photon. However, complete dissociation will occur after the absorption of two photons in agreement with the experimental findings.

energy with the dissociation energy. The branching ratio between the two processes was calculated as a function of the excitation energy (Fig. 8). Including a thermal energy before photoexcitation of 0.65 eV (298 K), the total excitation energy after two-photon absorption is 12.5 eV. Even at this high energy, the  $a^+(\text{CE})/[\text{Ala-Pro} + \text{H}^+]$  branching ratio is only  $2.5 \times 10^{-5}$ , which is far from the experimental number close to one. To reproduce the experimental ratio, it is necessary to reduce the reaction energy for the formation of  $a^+(\text{CE})$  and  $x$  to 2.35 eV. This is nearly 1 eV less than our calculated value.

Chen *et al.*<sup>23</sup> have done excited state calculations on simple model systems containing the amide moiety. They found that after excitation to the  $n\pi^*$  state ( $n$  is a lone pair electron on the amide oxygen), electronic deexcitation to the ground state is ultrafast *via* a conical intersection associated with elongation of the C–N bond and formation of a di-radical configuration. Interestingly, theory predicted that breakage of the C–N bond was competitive with internal conversion to the ground state,

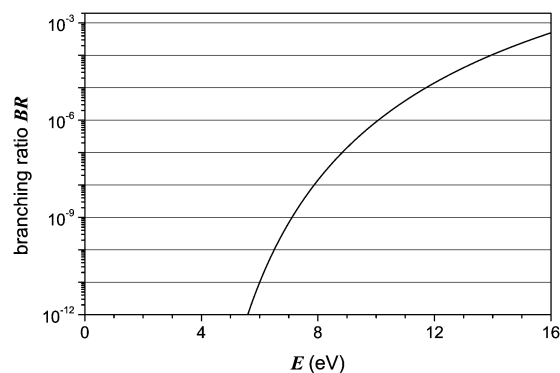


Fig. 8 Branching ratio between the loss of CE and the formation of  $a^+(\text{CE})$  versus excitation energy. Even after the absorption of two photons, the ratio is less than  $10^{-4}$  which implies that the formation of  $a^+(\text{CE})$  cannot compete with CE loss, and importantly not account for the large measured yield of  $a^+(\text{CE})$ , if randomization of the energy has time to occur before dissociation.

with almost equal probability while experiments by Keiding and co-workers<sup>24</sup> on formamide in solution showed that the hot molecule was predominantly formed. In solution dissipation of the excess energy to surrounding solvent molecules is ultrafast and competes with intramolecular vibrational redistribution of the energy. If C–N breakage accounts for the prompt dissociation observed in our work, fast loss of CO is subsequently required as  $a^+$  ions and not  $b^+$  ions were observed. More work is needed to fully understand the dissociation mechanism.

## Conclusions

In this work, we have provided additional evidence that the energy flow in peptides after 210 nm photoexcitation of the backbone is governed by two competing processes, either prompt dissociation occurs or the weakest bond is broken after internal conversion and intramolecular vibrational redistribution of the excess energy (statistical dissociation). Theoretical calculations of statistical rate constants strongly indicate that homolytic backbone cleavage is too slow to compete with CE loss (statistical process), basically due to a too large difference in dissociation energies. Hence only prompt dissociation can account for the high observed yield of backbone dissociation. Furthermore, all experimental observations made here and in previous work are in agreement with prompt dissociation. As the absorption cross section at 210 nm excitation wavelengths is higher for proline linkages than for other ones, our work demonstrates how PID provides some selectivity on where in the peptide backbone to induce cleavages. While prompt dissociation is significant, statistical dissociation dominates, which renders peptides quite photostable even at these high excitation energies. An important issue for future studies is how the geometrical structure influences the competition between the two processes.

## Acknowledgements

S. B. N. acknowledges support from the Danish Council for Independent Research (Grant No. 4181-000488). K. H. acknowledges grants from the University of Gothenburg Faculty of Science Strategic Initiative and from Aarhus Universitets Forskningsfond.

## Notes and references

- J. P. Reilly, *Mass Spectrom. Rev.*, 2008, **28**, 425.
- T. Ly and R. R. Julian, *Angew. Chem., Int. Ed.*, 2009, **48**, 7130.
- J. S. Brodbelt, *Chem. Soc. Rev.*, 2014, **43**, 2757.
- A. L. Sobolewski, W. Domcke, C. Dedonder-Lardeux and C. Jouvet, *Phys. Chem. Chem. Phys.*, 2002, **4**, 1093.
- S. R. Mercier, O. Boyarkin, A. Kamariotis, M. Guglielmi, I. Tavernelli, M. Cascella, U. Rothlisberger and T. R. Rizzo, *J. Am. Chem. Soc.*, 2006, **128**, 16938.
- G. Aravind, B. Klærke, J. Rajput, Y. Toker, L. H. Andersen, A. V. Bochenkova, R. Antoine, J. Lemoine, A. Racaud and P. Dugourd, *J. Chem. Phys.*, 2012, **136**, 014307.
- L. Joly, R. Antoine, M. Broyer, P. Dugourd and J. Lemoine, *J. Mass Spectrom.*, 2007, **42**, 818.
- J. A. Wyer, A. Ehlerding, H. Zettergren, M.-B. S. Kirketerp and S. Brøndsted Nielsen, *J. Phys. Chem. A*, 2009, **113**, 9277.
- H. T. H. Nguyen, C. J. Shaffer, R. Pepin and F. Turecek, *J. Phys. Chem. Lett.*, 2015, **6**, 4722.
- W. D. Bowers, S.-S. Delbert, R. L. Hunter and R. T. McIver, Jr., *J. Am. Chem. Soc.*, 1984, **106**, 7288.
- V. H. Wysocki, G. Tsaprailis, L. L. Smith and L. A. Breci, *J. Mass Spectrom.*, 2000, **35**, 1399.
- C. S. Byskov, F. Jensen, T. J. D. Jørgensen and S. Brøndsted Nielsen, *Phys. Chem. Chem. Phys.*, 2014, **16**, 15831.
- B. J. H. Kuipers and H. Gruppen, *J. Agric. Food Chem.*, 2007, **55**, 5445.
- K. Stöckel, B. F. Milne and S. Brøndsted Nielsen, *J. Phys. Chem. A*, 2011, **115**, 2155.
- J. A. Wyer and S. Brøndsted Nielsen, *Angew. Chem., Int. Ed.*, 2012, **51**, 10256.
- M. J. Frisch, G. W. Trucks, H. B. Schlegel, G. E. Scuseria, M. A. Robb, J. R. Cheeseman, J. A. Montgomery, Jr., T. Vreven, K. N. Kudin, J. C. Burant, J. M. Millam, S. S. Iyengar, J. Tomasi, V. Barone, B. Mennucci, M. Cossi, G. Scalmani, N. Rega, G. A. Petersson, H. Nakatsuji, M. Hada, M. Ehara, K. Toyota, R. Fukuda, J. Hasegawa, M. Ishida, T. Nakajima, Y. Honda, O. Kitao, H. Nakai, M. Klene, X. Li, J. E. Knox, H. P. Hratchian, J. B. Cross, V. Bakken, C. Adamo, J. Jaramillo, R. Gomperts, R. E. Stratmann, O. Yazyev, A. J. Austin, R. Cammi, C. Pomelli, J. W. Ochterski, P. Y. Ayala, K. Morokuma, G. A. Voth, P. Salvador, J. J. Dannenberg, V. G. Zakrzewski, S. Dapprich, A. D. Daniels, M. C. Strain, O. Farkas, D. K. Malick, A. D. Rabuck, K. Raghavachari, J. B. Foresman, J. V. Ortiz, Q. Cui, A. G. Baboul, S. Clifford, J. Cioslowski, B. B. Stefanov, G. Liu, A. Liashenko, P. Piskorz, I. Komaromi, R. L. Martin, D. J. Fox, T. Keith, M. A. Al-Laham, C. Y. Peng, A. Nanayakkara, M. Challacombe, P. M. W. Gill, B. Johnson, W. Chen, M. W. Wong, C. Gonzalez and J. A. Pople, *Gaussian 03, Revision D.01*, Gaussian, Inc., Wallingford CT, 2004.
- K. Hansen, *Philos. Mag. B*, 1999, **79**, 1413.
- T. Baer and P. M. Mayer, *J. Am. Soc. Mass Spectrom.*, 1997, **8**, 103.
- K. Hansen, *Statistical Physics of Nanoparticles in the Gas Phase*, Springer, Dordrecht, 2013.
- T. Beyer and D. R. Swinehart, *ACM Commun.*, 1973, **16**, 379.
- A. I. S. Holm, M. K. Larsen, S. Panja, P. Hvelplund, S. Brøndsted Nielsen, R. D. Leib, W. A. Donald, E. R. Williams, C. Hao and F. Turecek, *Int. J. Mass Spectrom.*, 2008, **276**, 116.
- L. Partanen, H. Vehkamäki, K. Hansen, J. Elm, H. Henschel, T. Kurtén, R. Halonen and E. Zapadinsky, *J. Phys. Chem. A*, 2016, **120**, 8613.
- X. Chen, L. Gao, W. Fang and D. L. Phillips, *J. Phys. Chem. B*, 2010, **114**, 5206.
- C. Petersen, N. H. Dahl, S. K. Jensen, J. Thøgersen and S. R. Keiding, *J. Phys. Chem. A*, 2008, **112**, 3339.